Electronic Supplementary Material (ESI) for Lab on a Chip.

Supporting information

A Semi-Dry Chemistry Hydrogel-Based Smart Biosensing Platform for On-Site Detection of Metal Ions

Xiaoxia Mao,[a,b,1] Dongsheng Mao,[a,1] Juanjuan Jiang,[c] Benyue Su,[d] Guifang Chen,[a,*] Xiaoli Zhu,[a,*]

[a] Center for Molecular Recognition and Biosensing, School of Life Sciences, Shanghai University, Shanghai 200444, P. R. China.

[b] Key Laboratory of Aqueous Environment Protection and Pollution Control of Yangtze River in Anhui of Anhui, Provincial Education Department, College of Resources and Environment, Anqing Normal University, Anqing 246011, P. R. China.

[c] College of Electrical Engineering, Anhui Polytechnic University, Wuhu 241000, P. R. China.

[d] School of Computing, Anqing Normal University, Anqing 246011, P. R. China.

[1] These authors contributed equally in this work.

* Corresponding author. gfchen@shu.edu.cn (G. Chen); xiaolizhu@shu.edu.cn (X. Zhu)

Table of contents

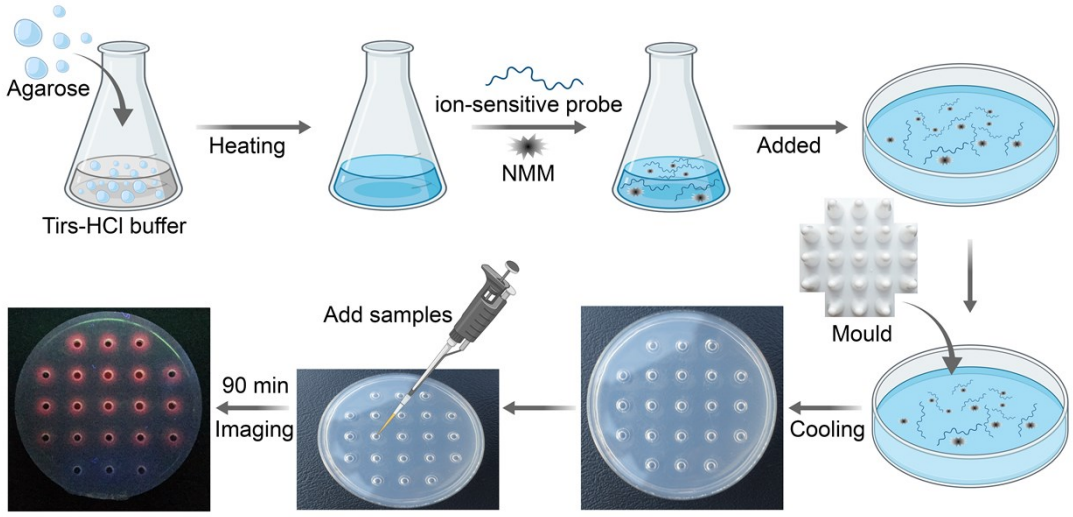

Figure S1 Schematic illustration of the preparation process of DNA incorporated agarose hydrogel and hydrogel-based analysis.

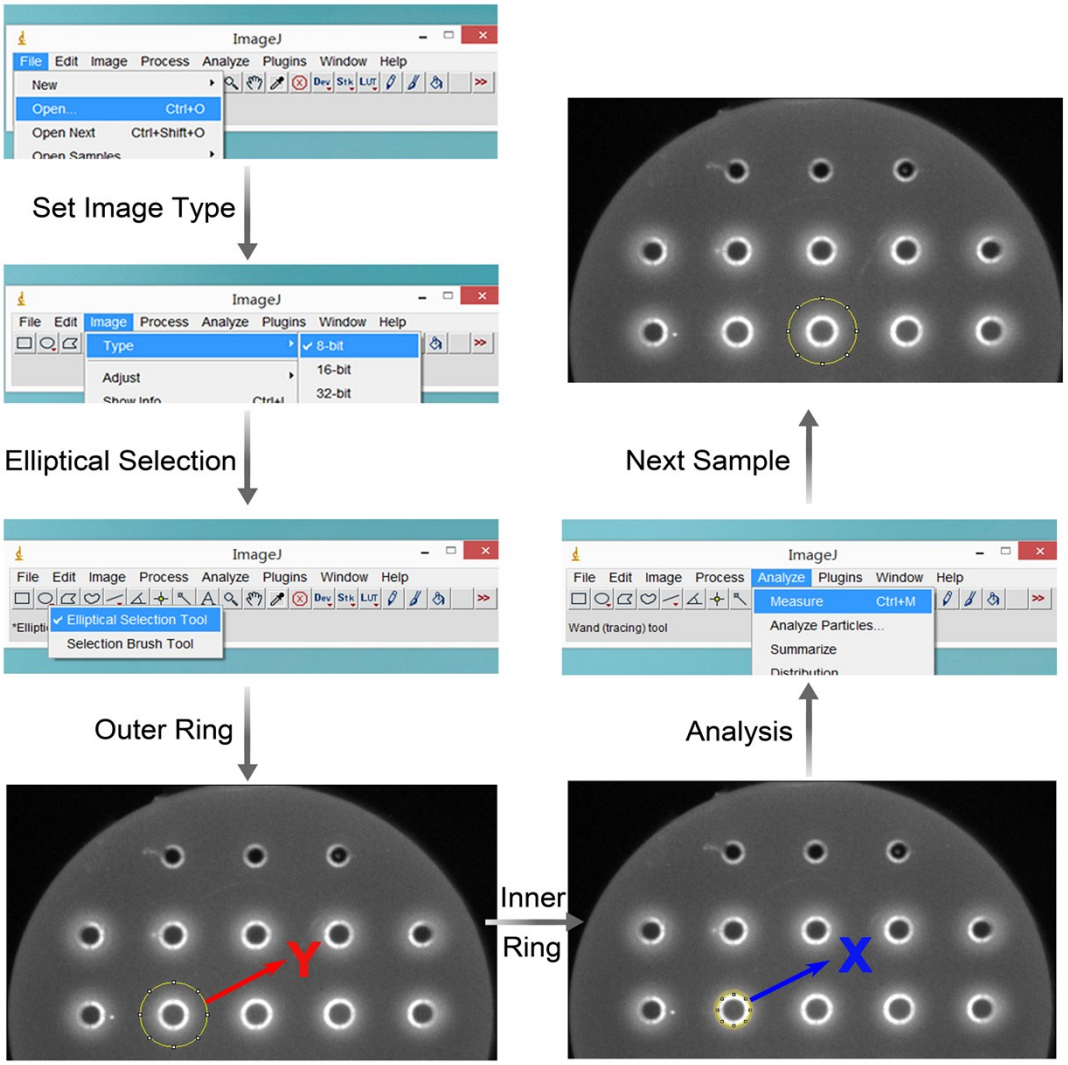

Figure S2 Manual analysis process by ImageJ software.

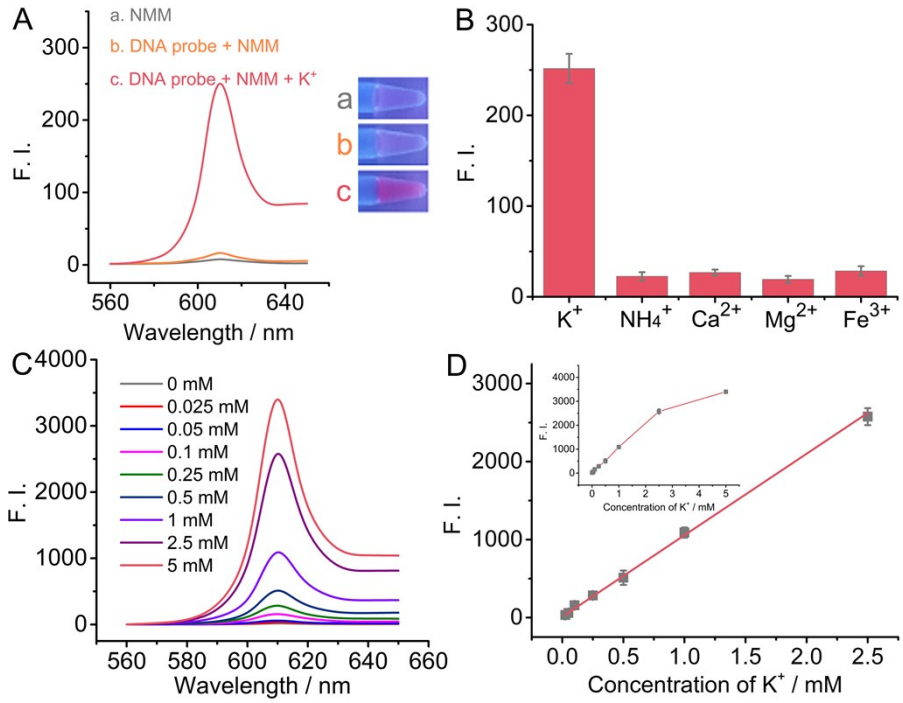

Figure S3 Feasibility of the fluorescent detection of K^+. (A) Fluorescence spectra of 100 mM Tris-HCl buffer solutions containing different reagents: NMM, NMM + DNA probe, and NMM + DNA probe + K^+, respectively (left part). And corresponding photographic images under UV light (right part). The concentration of NMM, DNA probe, and K^+ were 50 μM, 1.5 μM, and 0.25 mM, respectively. (B) Selectivity verification of K^+ detection. (C) Fluorescence spectra in the detection of different concentrations of K^+. (D) Linear relationship of the fluorescence intensity at 620 nm and the concentration of K^+. The inset shows the fluorescence intensity in the presence of different concentrations of K^+.

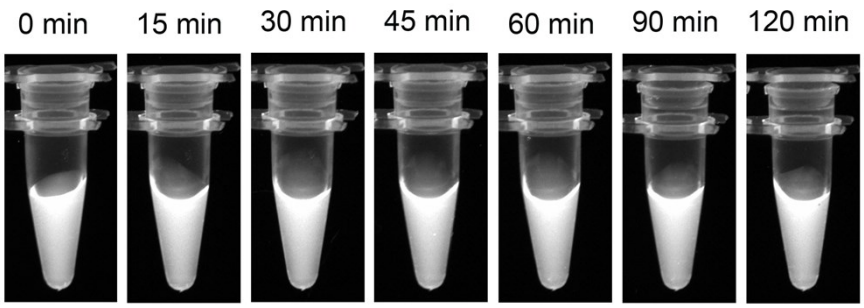

Figure S4 The stability of fluorescence signal of the reaction solution. 5 mM K^+, 1.5 μM DNA probe, and 50 μM NMM were reacted in 100 mM Tri-HCl (pH = 7.4) at 25 °C for 120 min.

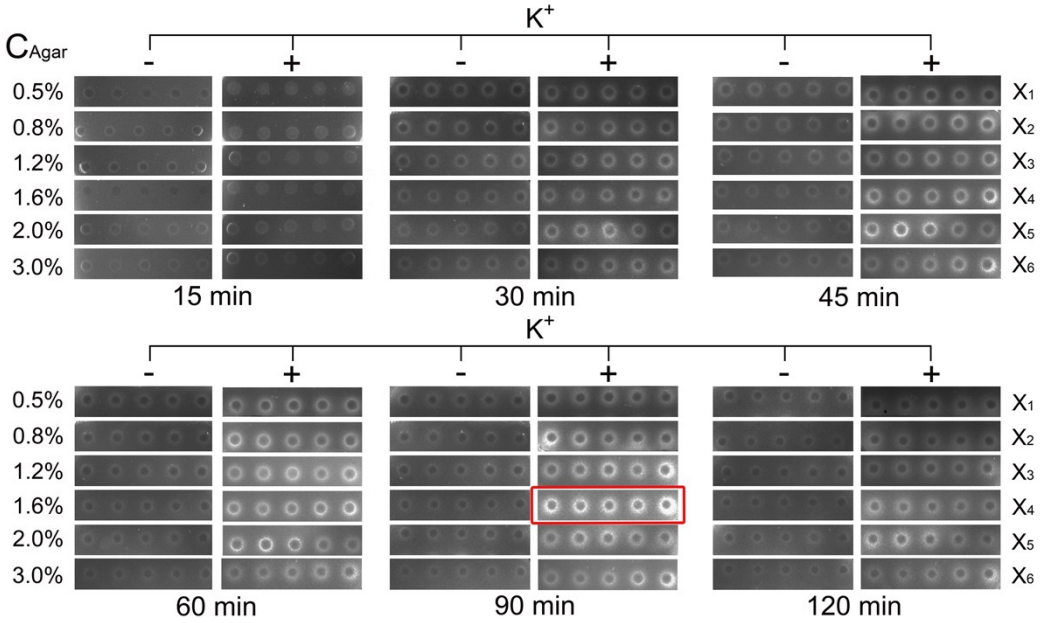

Figure S5 Effect of the concentration of agar on the fluorescence intensity. 5 mM K^+, 2 μM DNA probe, and 50 μM NMM were reacted in 100 mM Tri-HCl at 25 °C for 120 min.

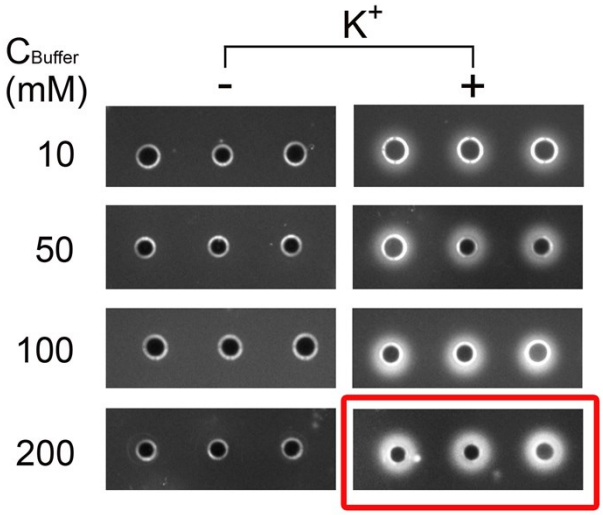

Figure S6 Effect of the concentration of buffer solution on the fluorescence intensity. 5 mM K^+, 2 μM DNA probe, and 50 μM NMM were reacted at 25 °C for 90 min.

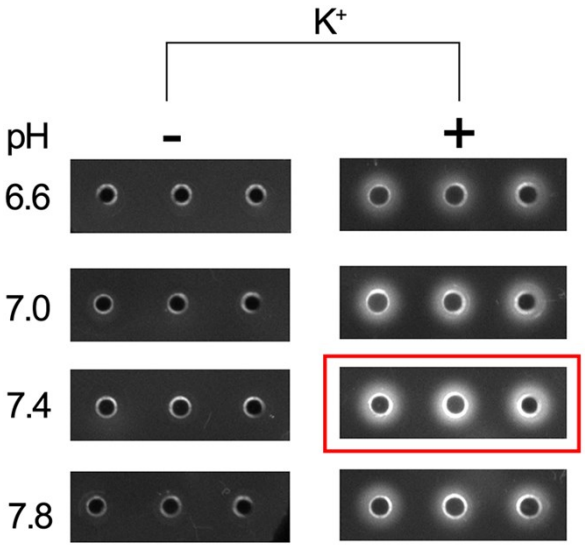

Figure S7 Effect of the pH values of buffer solution on the fluorescence intensity. 5 mM K^+, 2 μM DNA probe, and 50 μM NMM were reacted in 200 mM Tri-HCl at 25 °C for 90 min.

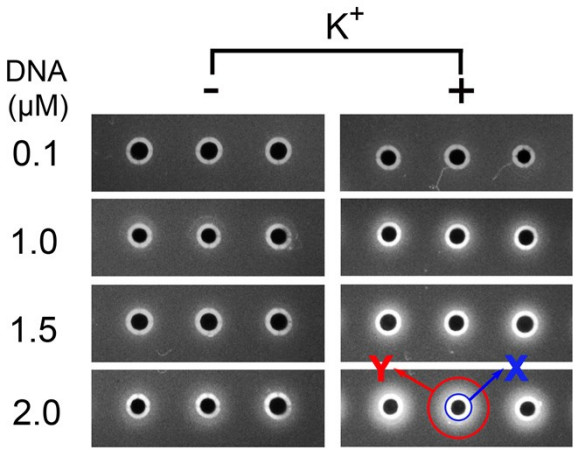

Figure S8 Effect of the concentration of DNA probe on the fluorescence intensity. 5 mM K^+ and 50 μM NMM were reacted in 200 mM Tri-HCl (pH = 7.4) at 25 °C for 90 min.

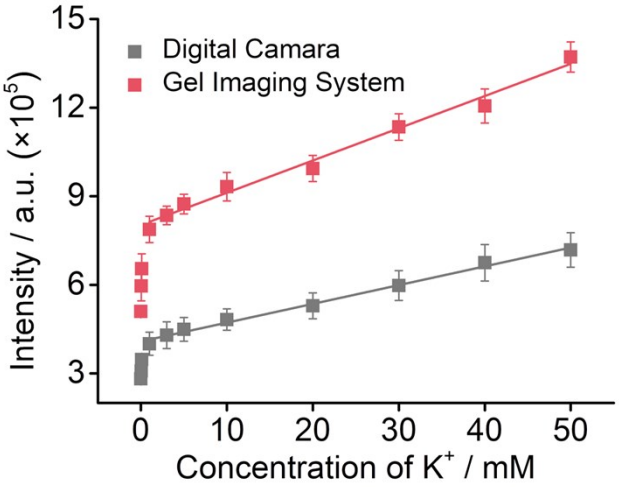

Figure S9 Linear relationship between the fluorescence intensity and the concentration of K^+. Data was acquired by manual analysis based on ImageJ software.

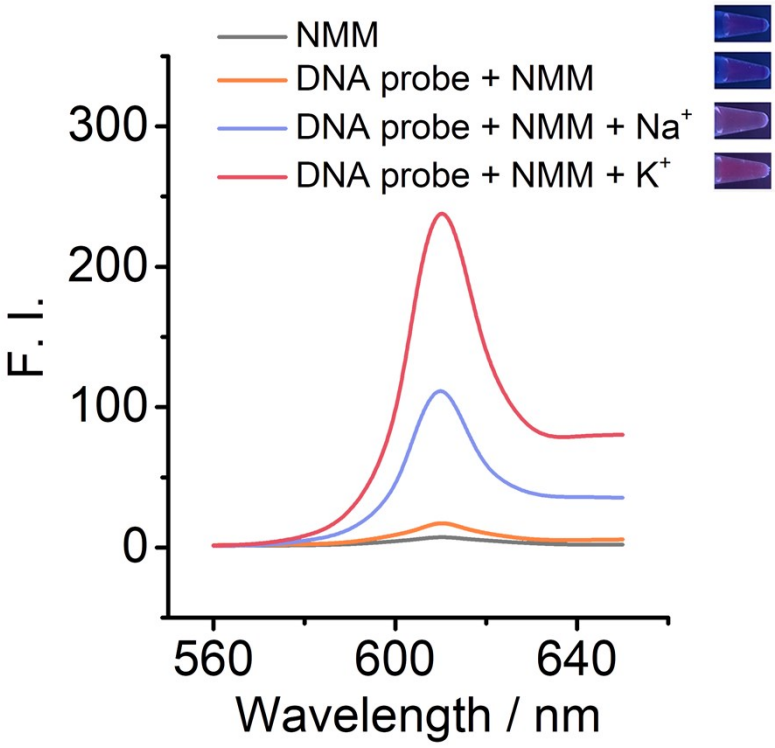

Figure S10 Comparison of the fluorescent detection of Na^+ and K^+ in solution. (A) Fluorescence spectra of 100 mM Tris-HCl buffer solutions containing different reagents: NMM, NMM + DNA probe, NMM + DNA probe + Na^+, and NMM + DNA probe + K^+, respectively (left part), and corresponding photographic images under UV light (right part). The concentration of NMM, DNA probe, Na^+ and K^+ were 50 μM, 1.5 μM, 0.25 mM, and 0.25 mM, respectively.

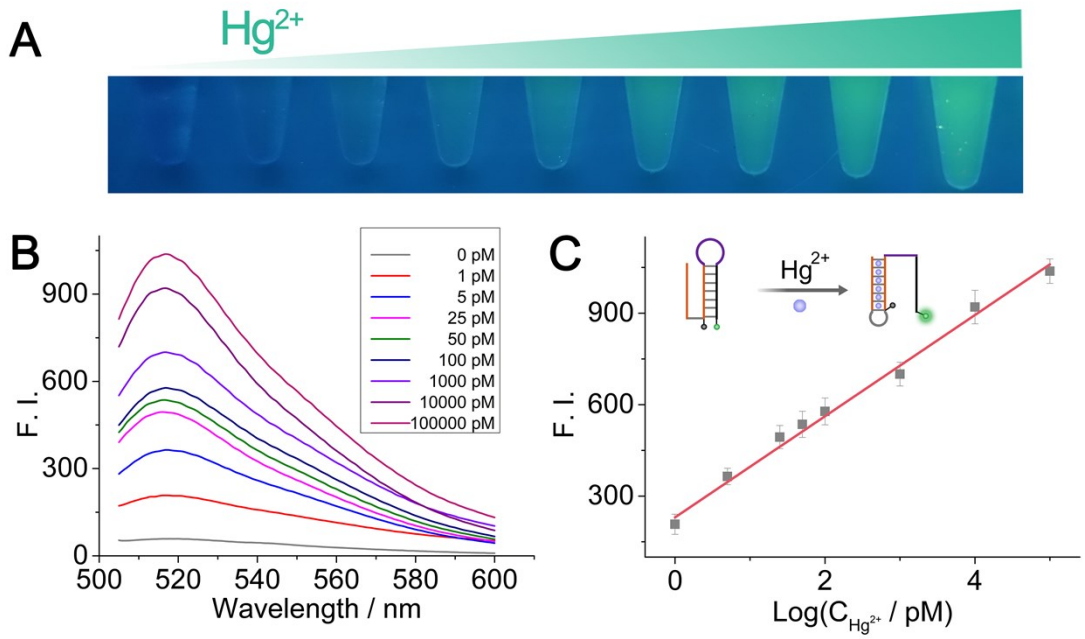

Figure S11 Feasibility of the fluorescent detection of Hg^{2+} based on Hg^{2+}-sensitive DNA probe. (A) Photographic images of the detection of different concentrations of Hg^{2+} under UV light. (B) Fluorescence spectra in the detection of different concentrations of Hg^{2+}. (C) Linear relationship of the fluorescence intensity at 520 nm and the concentration of Hg^{2+}. The inset shows the allosteric switch of the DNA probe in the presence of Hg^{2+}.

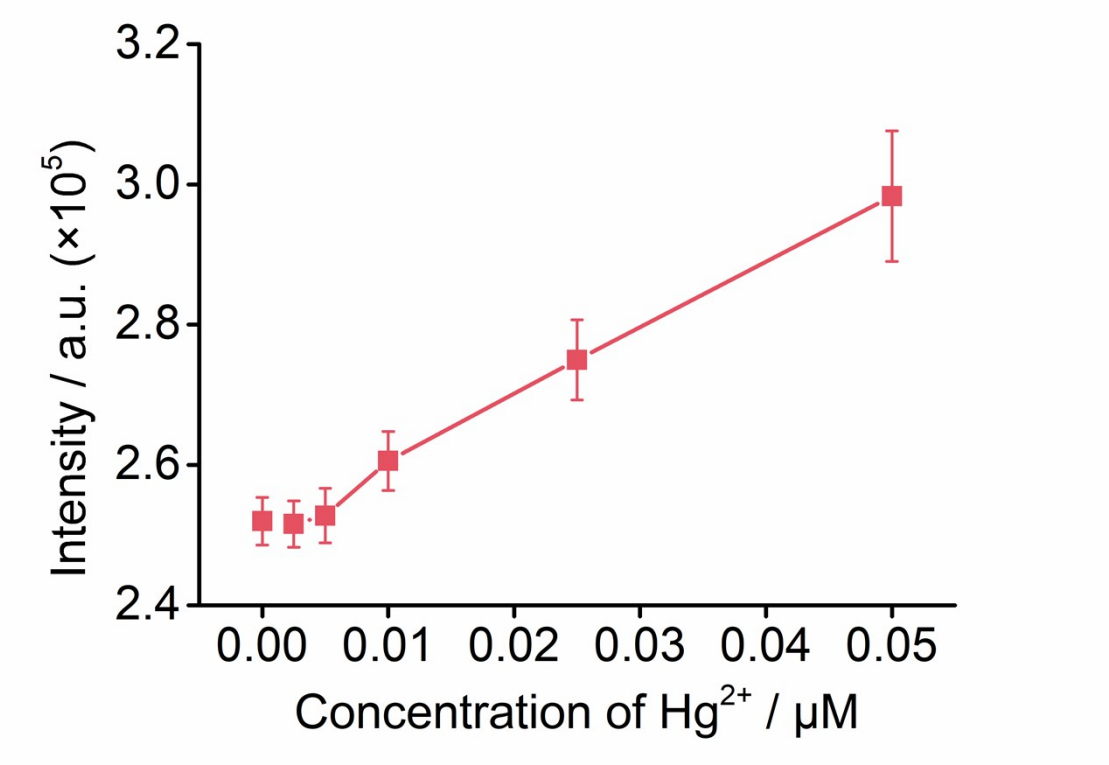

Figure S12 Linear relationship between the fluorescence intensity and the concentration of Hg^{2+}. Data was acquired by manual analysis based on ImageJ software.

Table S1 The comparison of detection performances of our method and other methods in the detection of K^+.

Method	Limit of detection	Linear range	Reference
Pyrene-labeled G-quadruplex oligonucleotide	1 mM	2 mM ~ 10 mM	[1]
DNA/aptamer-based optical biosensors	0.4 mM	0.6 mM ~ 20 mM	[2]
G-quadruplex-specific fluorescent probe	0.5 mM	2 mM ~ 20 mM	[3]
DNA hydrogel-based plate	0.34 mM	1 mM ~ 40 mM	This work

Table S2 The comparison of detection performances of our method and other methods in the detection of Hg^{2+}.

Method	Limit of detection	Linear range	Reference
Carbon quantum dots/3-aminophenylboronic acid Hybrid	38.1 nM	0.1 μM ~ 6.0 μM	[4]
Cellulose nanofiber substrate-supported luminescent gold nanoparticles	1 nM	1 nM ~ 1 mM	[5]
Hollow AuAg nanocages	10 nM	30 nM ~ 35 μM	[6]
Mercury-stimulated Ag_3PO_4 microcubes	20 nM	0.1 μM ~ 7 μM	[7]
DNA hydrogel-based plate	5.6 nM	10 nM ~ 2.5 μM	This work

References

1 S. Nagatoishi, T. Nojima, B. Juskowiak, S. Takenaka. *Angew. Chem.* 2005, **44**, 5067–5070.

2 C. Shi, H. X. Gu, C. P. Ma. *Anal. Biochem.* 2010, **400**, 99–102.

3 T. Li, E. K. Wang, S. J. Dong. *Anal. Chem.* 2010, **82**, 7576–7580.

4 H. Wu, C. Tong. *Anal. Chem.* 2020, **92**, 8859–8866.

5 J. Fu, J. Zhu, Y. Tian, K. He, H. Yu, L. Chen, D. Fang, D. Jia, J. Xie, H. Liu, J. Wang, F. Tang, J. Tao, J. Liu. *Sensor. Actuat. B: Chem.* 2020, **319**, 128295.

6 J. Chen, S. Zhao, J. Zhu, J. Li, J. Zhao. *J. Alloy. Compd.* 2020, **828**, 154392.

7 Y. Zhang, P. Ju, L. Sun, Z. Wang, X. Zhai, F. Jiang, C. Sun. *Microchim. Acta.* 2020, **187**, 422.